**HEFAT2012**
**9th International Conference on Heat Transfer, Fluid Mechanics and Thermodynamics**
**16 – 18 July 2012**
**Malta**

# CHARACTERISTICS OF OXYFUEL AND AIR FUEL COMBUSTION IN AN INDUSTRIAL WATER TUBE BOILER

R. Ben-Mansour*, M.A. Habib, M. Rajhi, M. NemitAllah, K. A. Suara
*Author for correspondence
Department of Mechanical Engineering,
King Fahd University of Petroleum and Mineral,
Dhahran, Saudi Arabia,
E-mail: rmansour@kfupm.edu.sa

## ABSTRACT

The characteristics of oxyfuel combustion are compared to those of air-fuel combustion in the furnace of a typical industrial water tube boiler. Two oxyfuel cases are considered. These correspond to 21% $O_2$ and 29% $O_2$ by volume. Validations for both oxyfuel combustion and air-fuel combustion indicate that the temperature levels are reduced in oxyfuel combustion. The results show that, as the percentage of recirculated $CO_2$ is increased, the temperature levels are greatly reduced. It is concluded that the flame propagation speed in $O_2/CO_2$ environment is lower than that in $O_2/N_2$. It is found that the fuel and oxygen consumption rates are slower in oxyfuel combustion relative to air-fuel combustion. Heat transfer from the burnt gases to the water jacket along the different surfaces of the furnace is calculated. It is shown that the energy absorbed is much higher in the case of air-fuel combustion along all surfaces except for the end part of the furnace close to the furnace rear wall.

***Keywords***: Computational fluid dynamics; Oxyfuel combustion; Air-fuel combustion;; Water tube boilers, Industrial boilers.

## INTRODUCTION

Greenhouse gas emissions from energy production can be reduced through the use of alternative energy sources such as nuclear power and renewable energy. Renewable energy sources are increasingly used, however, until these sources can reliably and cost-effectively produce significant amounts of energy, the immediate energy demand is likely to be met by combustion of fossil fuels [IEA (2004) and WEC (2004)]. Carbon capture is essential to enable the use of fossil fuels while reducing the emissions of $CO_2$ into the atmosphere. The development of $CO_2$ capture technologies for hydrocarbon fired power plants is proceeding along several fronts including separation of $CO_2$ from waste gas (post-combustion decarbonization), combustion in $O_2$ instead of air (oxyfuel combustion) and production of a carbon-free fuel (pre-combustion decarbonization) [Wall (2007)]. Among the methods of $CO_2$ capture and storage, oxyfuel technology provides a promising option for power and steam generation systems. In this technology, the fuel is burned in pure oxygen instead of air, and the flue gas consists primarily of $CO_2$ and $H_2O$ that can be easily separated via condensation. In order to provide the ballasting effect of the absent $N_2$ and moderate the furnace temperature, a fraction of the flue gas is recycled in the combustion chamber [Buhre et al. (2005) and Zhang and Lior (2008)].

Several factors affect the efficiency of oxyfuel combustion system [Rising, 2007] including: 1) the performance of the air separation unit, 2) the compression and purification of $CO_2$, 3) working fluid temperature and 4) turbine cooling load, [Sanz et al. (2005), Kvamsdal (2005), Wall (2007) and Normann et al. (2009)]. Shah and Kristie (2007) made a comparison between the performance of a boiler utilizing oxyfuel combustion and another boiler utilizing air combustion and having a net power output of 452 MW. They reported an efficiency reduction from 44% to 34.7% and a reduction of $CO_2$ emission from 8632 to 1132 tons per day. Buhre et al. (2005) reviewed research on the oxyfuel combustion technology, focusing mainly on oxyfuel combustion of pulverized coal. They showed that oxyfuel combustion has the advantage of smaller flue gas cleaning equipment as well as retrofits of existing plants. Buhre et al. (2005) identified four important issues; namely 1) heat transfer, 2) gaseous emissions, 3) ash-related issues, and 4) ignition and flame stability of the combustion. They have also identified the research needs including the heat transfer performance of new and retrofitted plants, impact of oxygen feed concentration and $CO_2$ recycle ratio, assessment of retrofits for electricity cost and cost of $CO_2$ sequestration, combustion in an $O_2/CO_2$ environment including ignition, burn-out, and emissions.

$CO_2$ and $H_2O$ have higher emissivity which produces more radiation. On the other hand, carbon dioxide and water vapor have high heat capacities compared to nitrogen. This increase in thermal capacity causes an increase in heat transfer in the convection sections. Kakaras et al. (2007) investigated radiative heat transfer in oxyfuel combustion for low-grade quality fuels. Flue gas recirculation was required in combustion to moderate the furnace temperature, due to the absence of $N_2$. Similar combustion temperatures were

maintained in both cases. They investigated the impact of oxy-combustion on the design of heat exchange surfaces and found that higher radiative heat transfer (due to the high concentrations of $CO_2$ and $H_2O$ in the flue gas) and flue gas mass flow rate. Most of the previous work on oxyfuel combustion focused on coal. Andersson et al. (2007a) and Andersson and Johnsson (2006) compared radiative heat transfer in oxyfuel flames and air-fuel flames during combustion of lignite. They used the same stoichiometry for all cases, and adjusted the flue gas recycle rate in the oxyfuel combustion process. They measured the radial profiles of gas concentration, temperature and total radiation intensity in the furnace. In another study, Andersson et al. (2007b) presented their results on the differences in soot-related radiation intensity between two different oxyfuel flame and air-fired flame. The study was conducted in a 100 kW oxyfuel test unit firing propane while keeping an oxygen-to-fuel ratio of 1.15. They indicated that carbon dioxide not only increases the gas radiation, but it can also drastically change the radiation originating from soot during oxyfuel combustion. Investigation of the feasibility of hydroxyl-fuel combustion for the oxyfuel systems was performed by Zanganeh et al. (2007). Modeling and pilot-scale experiments were carried out in order to study the reduction in size and capital cost of equipment of such systems. In addition, the possibility of using water/steam to moderate the flame temperature was considered.

The fundamentals of the oxyfuel combustion for gas and coal firing in a 100 kW oxyfuel test facility were studied experimentally and theoretically by Andersson (2007). The results showed that the temperature level of the flame (using 27% $O_2$ and 73% $CO_2$ and a swirl number of 0.79) drops drastically and leads to a delayed burn-out compared to the normal air-fuel flames. It is observed higher emissivity and attributed this to the increase in gas band radiation as well as the rise in the soot volume fraction. Shaddix (2007) studied the combustion behavior and ignition of individual coal particles in 6-36% $O_2$ in $N_2$ and in $CO_2$ at 1400 to 1800 K. He found that, for combustion in $CO_2$ environment, flame temperatures were reduced significantly (from 2226 K to 1783 K). He concluded that $CO_2$ appeared to decrease char burning rate. Similar results have been found in other experimental and theoretical investigations of other oxyfuel flames [Wall et al. (2007)]. In oxyfuel combustion, oxygen in the near burner region can increase flame stability, an advantage in high velocity burners. Ditaranto and Hals (2007) investigated the thermo-acoustic instabilities in a $CO_2$ diluted oxyfuel combustor and showed that additional control of $CO_2$ dilution/ $O_2$ enrichment allows more possibilities for "zoning" the flame. It was also found that the increase in burner stability by oxygen enrichment can lead to an increase of dynamic instability. Therefore, staging $O_2$ to enhance combustor performance should be done carefully. It was concluded that knowledge of flame properties in $CO_2/O_2$ system was necessary to predict the flame structure. The potential changes in flame stability and pollutant formation were also noted by other researchers [Croiset and Thambimuthu (1999) and Payne (1989)].

Carbon dioxide and water vapor have high thermal capacities compared to nitrogen [Buhre et al. (2005)]. This increase in thermal capacity increases the heat transfer in the convective section of the boiler. However, the less amount of gas passing through the boiler in the oxyfuel case combined with the increased heat transfer in the radiative section results in lower gas temperatures entering the convective pass. Both of these factors lead to lower heat transfer in the convective section of the boiler. However, for a retrofit where furnace heat transfer is matched with a given flue gas oxygen concentration, the oxyfuel case will result in a lower furnace exit gas temperature [Khare et al. 2005].

CFD is a powerful tool for providing details of the velocity, temperature and concentration variations that are not easily obtained through experimental measurements. Eriksson (2007) adapted CFD software packages to oxyfuel combustion with the objective of developing gas phase reaction schemes, measurement of soot in oxyfuel combustion and development of soot model and coal characterization under oxyfuel conditions. Eriksson (2007) indicated that the development and validation of the submodels were necessary for oxyfuel conditions and that detailed measurement data from well defined flames in different scale are needed as validation data. Yang et al. (2003) investigated the performance of Reynolds turbulence model for numerical study of non reacting gas turbine combustor swirl flow. Mean velocities and Reynolds shear stress were presented. Mongia (2008) presented the progress made in comprehensive modeling of gas turbine combustion. Computational Combustion Dynamics (CCD) codes were developed to assess empirical/analytical design methodology for low emission combustion systems.

The above literature review indicated that most of the previous results were focused on coal combustion. As well, the influence of replacing $N_2$ in air-fuel combustion by $CO_2$ in oxyfuel combustion on the flame and gas properties and on the temperature levels and absorption by boiler water walls in general and in gaseous fuel combustion in particular are not clearly known.

## MATHEMATICAL FORMULATION

### The General Form of The Governing Equations

The equations which govern the conservation of mass, momentum and energy as well as the equations for species transport may be expressed in the following general form (Reynolds, 1987 and Shih et al, 1995):

$$\frac{\partial}{\partial x_j}\left(\bar{\rho}\,\bar{U}_j\Phi + \bar{\rho}\,\overline{u_j\phi}\right) = \frac{\partial}{\partial x_j}\left[\Gamma_\phi \frac{\partial \Phi}{\partial x_j}\right] + \bar{\rho}\,S_\Phi \qquad (1)$$

where $\Phi$ and $\phi$ are the average and fluctuating values of the dependent variable and $u_j$ is the velocity component along the coordinate direction $x_j$, $\bar{\rho}$ is the fluid density, $\Gamma_\Phi$ is the diffusion coefficient and $S_\Phi$ is the source term.

Equation (1) stands for the mass conservation equation when $\Phi$ = 1; the momentum conservation equation when $\Phi$ is a velocity component; the energy equation when $\Phi$ is the stagnation enthalpy; or the transport equation of a scalar when $\Phi$ is a scalar variable such as mixture fraction. The present work utilizes the K-$\varepsilon$ model of Versteeg and Malalasekera (1995). The Reynolds stresses and turbulent scalar fluxes are related to the gradients of the mean velocities and scalar variable, respectively, via exchange coefficients as follows [Versteeg and Malalasekera (1995)]:

$$-\rho\overline{u_i u_j} = \mu_t\left(\frac{\partial \overline{U}_i}{\partial x_j}+\frac{\partial \overline{U}_j}{\partial x_i}\right)-\frac{2}{3}\rho k\delta_{ij} \tag{2}$$

$$-\rho\overline{u_j\phi} = \Gamma_\Phi\frac{\partial \Phi}{\partial x_j} \tag{3}$$

where $\mu_t$ is the turbulent viscosity and $\Gamma_\Phi$ is equal to $\mu_t/\sigma_\Phi$. The turbulent viscosity is modeled as

$$\mu_t = c_\mu\,\rho\,k^2/\varepsilon \tag{4}$$

where $c_\mu$ and $\sigma_\Phi$ are constants. The turbulent viscosity is thus obtained from the solution of the transport equations for K and $\varepsilon$. RNG (Renormalized group) turbulence model [Wilcox (2000)] was used to provide better results for vertical flows. The eddy dissipation model that described turbulence-chemistry interaction in non-premixed combustion [Magnussen and Hjertager (1976)] was utilized in the present work to provide the production rate of species. The solution of the radiative transfer equation (RTE) was obtained using the discrete ordinates (DO) radiation model [Raithby and Chui (1990)]. The blackbody spectral emissive power is calculated using variables by Liu et al. (1998) and Zheng et al. (2000) based on expressions of Modak (1979) and Smith et al. (1982).

**Species Transport Equations**

The mass fraction of each species $m_l$, is predicted through the solution of a convection-diffusion equation for the $l^{\text{th}}$ species. The present calculations utilize a one step reaction model and solve transport equations for the species of $O_2$, $CO_2$ and $H_2O$. The conservation equations can be expressed in the following form:

$$\frac{\partial}{\partial x_i}(\rho\overline{U}_i\, m_l) = -\frac{\partial}{\partial x_i}J_{l,i}+R_l \tag{5}$$

where $R_l$ is the mass rate of creation or depletion by chemical reaction of the species l, $J_{l,i}$ is the diffusion flux of species l, which arises due to concentration gradients which is given by:

$$J_{l,i} = -(\rho D_{l,m}+\frac{\mu_t}{Sc_t})\frac{\partial m_l}{\partial x_i}$$

where $D_{l,m}$ is the diffusion coefficient for species l in the mixture and $Sc_t$ is the turbulent Schmidt number, $\frac{\mu_t}{\rho D_t}$ is equal to 0.7.

An eddy-dissipation model (Magnussen and Hjertager (1976)] that relates the rate of reaction to the rate of dissipation of the reactant- and product-containing eddies is used to calculate the rate of reaction.

**Radiation Heat Transfer Modeling**

In order to correctly predict the temperature distribution in the furnace a radiative transfer equation (RTE) for an absorbing, emitting and scattering medium has to be solved. The RTE equation is written as:

$$\frac{dI(\mathbf{r},\mathbf{s})}{ds} = \kappa I_b-(\kappa+\sigma_s)I(r,s) \tag{6}$$

The total radiation intensity I, depends on the position vector, *r*, and the path length s. κ is the absorption coefficient and $\sigma_s$ is the scattering coefficient. The Planck mean absorption coefficient is given as [Siegel and Howell (2002)]:

$$\kappa_P(T,P) = \frac{\int_0^\infty \kappa_\lambda(\lambda,T,P)e_{b\lambda}(\lambda,T)d\lambda}{\sigma T^4} \tag{7}$$

where $e_{b\lambda}$ is the blackbody spectral emissive power. κ is calculated using variables by Liu et al. (1998) based on expressions reported by Modak (1979).

**Boundary Conditions**

The velocity distribution is uniform at the inlet section with the velocity in the direction of the burner nozzle axis. Kinetic energy and its dissipation rate are selected such that $\sqrt{K/\overline{U}^2}=0.1$ and a length scale, L, equal to the characteristic length of the inlet pipe/annulus. At the wall boundaries, all velocity components are set to zero. Kinetic energy of turbulence and its dissipation rate are determined from the equations of the turbulence model. Constant wall temperature corresponding to saturated water temperature in the tube wall of the actual boilers was considered. The production of kinetic energy and its dissipation rate at the wall-adjacent cells are computed on the basis of the local equilibrium hypothesis. Under this assumption, the production of k and its dissipation rate are assumed to be equal in the wall-adjacent control volume. The ε-equation is not solved at the wall-adjacent cells. Thus, the production of k at the node close to the wall is taken proportional to the square of the wall shear stress. The rate of dissipation, ε, at the node close to the wall is proportional to $k^{3/2}$ [Versteeg and Malalasekera, 1995]

**Solution Procedure**

The set of governing equations and boundary conditions are solved numerically. The details of the calculation procedure can be found in previous works such as Habib and Whitelaw (1982), Attya and Habib (1990), Shuja and Habib (1996) and

Habib et al. (1989). Fluent was used to perform the calculations. A mesh of more than 1,000,000 finite volumes was used and the solution was considered converged when the summation of the residual in the governing equation summed at all domain nodes was less than 0.01%. In order to minimize the diffusion errors, the grids were concentrated in the regions of high gradients. A one-step chemical reaction model is used. The solution procedure solves the partial differential equations for conservation of mass, momentum and energy and combustion species. On the other hand, the boundary conditions for the calculation inside the furnace use a constant temperature boundary condition. This temperature is the saturation temperature corresponding to the boiler pressure.

**Validation**

Validations of the present computational model for the cases of air-based combustion and oxyfuel combustion were performed by comparing the predicted results with the experimental data of Andersson and Johnsson (2007). The combustion chamber in this case is shown in Fig. 1. Fuel is introduced in the central jet, surrounded by two annular oxidizer jets, a primary stream and a secondary stream. Both streams could be subjected to swirl, as described next. The oxidizer streams were either air or a mixture of $CO_2$ and $O_2$. The operating parameters are given below.

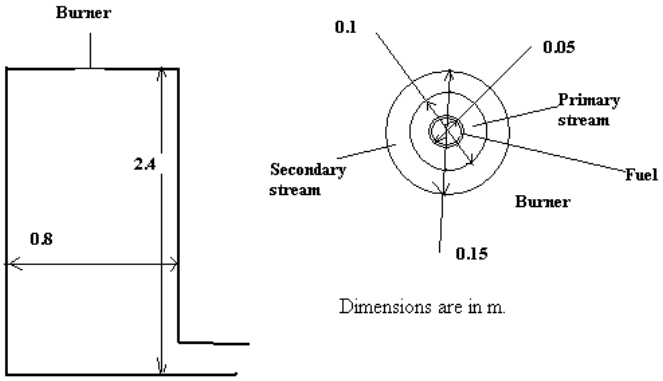


Figure 1 Experimental $O_2/CO_2$ combustion Unit [Andersson and Johnsson (2007)]

Fuel: Propane, with mass flow rate = 0.001726 kg/s, and temperature $T_{in}$ = 300 K

Case A

Primary stream: Air flowing at a rate of 0.0126 kg/s with swirl angle=45°, the air inlet temperature is $T_{in}$ = 300 K

Secondary stream: Air flowing at a rate of 0.0188 kg/s, swirl angle=15°, $T_{in}$ = 300 K

Case B

Primary stream: $O_2/CO_2$ mixture ($O_2$, 21%; $CO_2$, 79% by volume)

Secondary stream: $O_2/CO_2$ mixture ($O_2$, 21%; $CO_2$, 79% by volume)

The radial distributions of the temperature are shown in Figs. 2 and 3. The radial temperature profiles at 0.046 m shown for the air-based and oxyfuel-based combustion cases show a good agreement between predicted and experimental data, although few measurements are available.

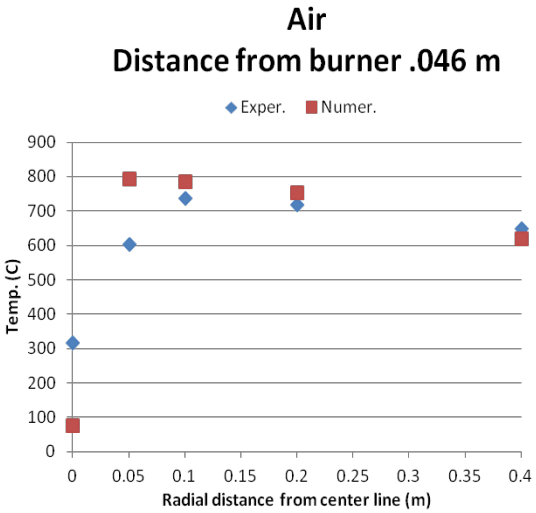


Figure 2 Experimental vs. numerical Temperature profile at distance .046 m from burner, air case

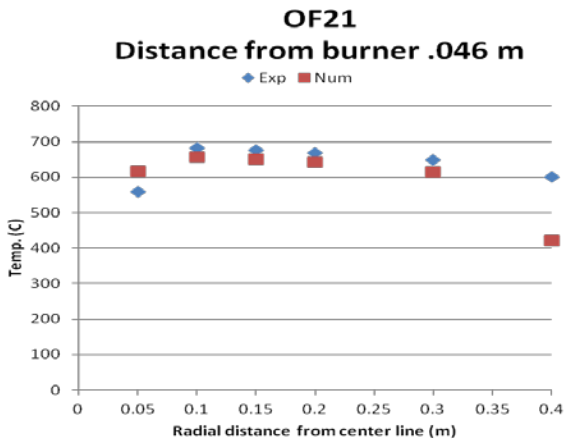


Figure 3 Experimental vs. numerical Temperature profile at distance .046 m from burner, OF21 case

**RESULTS**

The computational model was applied to the case of an industrial natural-gas-fired boiler to analyze the impact of replacing air with a mixture of $O_2$-$CO_2$.

**Boiler Description**

Results depicting the fluid flow, combustion characteristics and heat flux inside a typical package water tube boiler at full load are now presented. The boiler is of natural-circulation type and the three-dimensional view of the boiler furnace is shown in Fig. 4. The figure also shows the Cartesian coordinate system used in this study. The boiler uses natural gas as a fuel and has 6 burners on two levels (three burners in each level) located in the front wall (burner wall). The D-type tubes extend from the

mud drum (lower drum) through the bottom wall and form the burner wall. The top part of the D-shaped tubes forms the top wall of the furnace and ends at the upper drum. The tubes forming the bottom wall are thermally insulated. Tubes on the front wall extend from lower to upper drum while the tubes forming the side walls extend from a lower header to an upper header. The water-steam mixture inside the tube is normally saturated and has a saturation temperature corresponding to the drum pressure. Accordingly, the front, side, rear and top walls of the furnace provide a constant temperature boundary condition. The fuel is introduced through the nozzles surrounded by the primary air. The primary air is given a tangential component using 45° swirl angle (equivalent to swirl number of 0.58). The secondary air flows around the primary air nozzles with no swirl component. The mass flow rates of the primary and secondary air streams are 8.864 and 10.63 kg/sec, respectively. The boiler is of the package type and has a firing rate of 298 MW with a drum pressure of 52 atm. and steam flow rate of 94.7 kg/s.

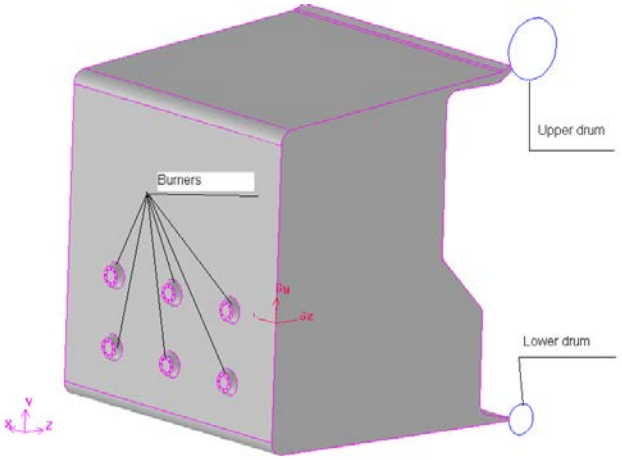


Figure 4 Three-dimensional view of a typical package boiler.

**Characteristics Of Oxyfuel And Air-Fuel Combustion Processes**

The influence of $CO_2$ circulation on the characteristics of the oxyfuel combustion process was investigated by considering two circulation ratios and comparing the results with the case of air-fuel combustion. The first case has 21% $O_2$ by volume while the second case has a mixture containing 29% $O_2$ by volume. Figure 5 shows a comparison between the temperature contours of the air-fuel case and the two oxyfuel combustion cases. The contours are shown in a vertical plane passing through the axes of the two burners. Figures 5a and 5b show that the temperature levels are close in both cases of air-fuel and 29 % combustion processes. This is expected based on the selected mass fraction of oxygen in the $O_2$-$CO_2$ mixture of 29 %. However, as $CO_2$ mass percentage is increased, the temperature levels are reduced, as indicated by Fig. 5c. We also note that the flame length increases in the case of oxyfuel combustion as compared to that of air-fired combustion. It appears that the combustion rate is slower when $N_2$ is replaced by $CO_2$, and is further slowed downstream leading to extending the burning zone. This can be clearly seen by comparing Figs 5a and 5c. The slower temperature rise observed in the oxyfuel combustion cases is attributed to the higher specific heat of $CO_2$. The figures also show that air combustion leads to a more compact hot flame while oxyfuel combustion produces a longer "milder" flame distributed over much of the combustion chamber length.

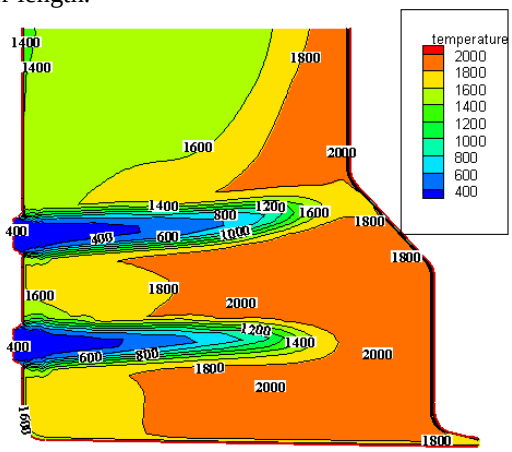


(a) Air-fuel combustion

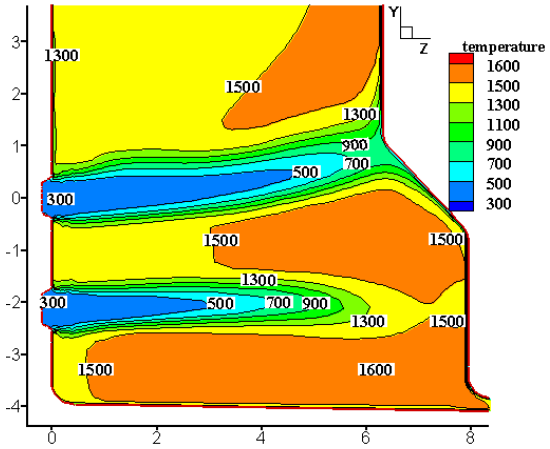


b) Oxyfuel combustion (21%$O_2$ and 79% $CO_2$ by volume)

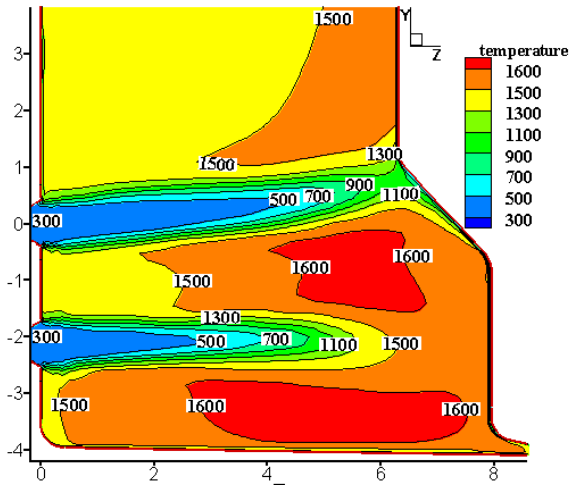


c) Oxyfuel combustion (29%O2 and 71% CO2 by volume)

Figure 5 Contours for temperature of vertical plane passing through burners 2 & 5

Further insight into the impact of $CO_2$ and the lower temperature levels in the case of oxyfuel combustion is gained by examining the contours of the fuel mole fraction in the three cases, as presented in Fig. 6. The contours are plotted in a vertical plane passing through the two middle burners. As shown in Fig. 6, the fuel burning rate is slower in the oxyfuel combustion cases in comparison to the air-fuel combustion case. It is also shown that the increase in the percentage of $CO_2$ results in further reduction in the fuel burning rate. Both observations are consistent with the trends in the temperature distribution discussed earlier. In order to shed some more light on the impact of oxyfuel combustion on the burning rate, the turbulent viscosity for the cases of air-fuel combustion and oxyfuel combustion were calculated. These results are shown in Fig. 7a, depicting the distribution of the turbulent viscosity along the axes of the lower middle burners. The figure indicates lower turbulent viscosity and hence slower mixing rates in the case of the oxyfuel combustion in comparison to those of air-fuel combustion, although the difference is small. Slower mixing rates between fuel and oxygen in the case of oxyfuel combustion reduces the combustion rate. The figure also shows higher turbulent viscosity for the oxyfuel case towards the furnace exit, reflecting higher combustion rates in that region and leading to high temperature levels as indicated in Fig. 5.

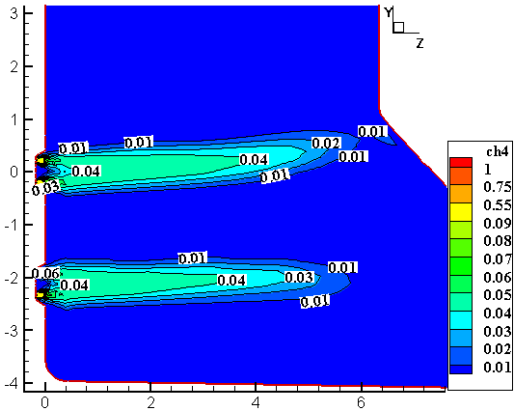


(a) Air-fuel combustion

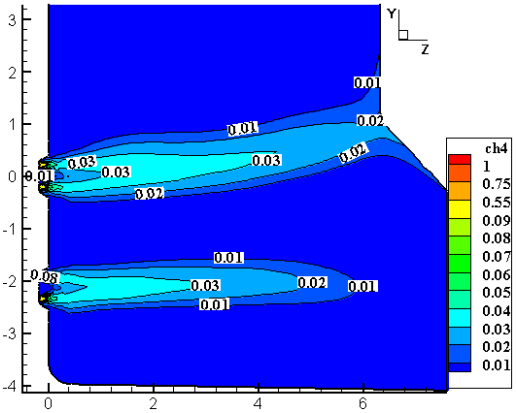


(b) Oxyfuel combustion (21%O2 and 79% CO2 by volume)

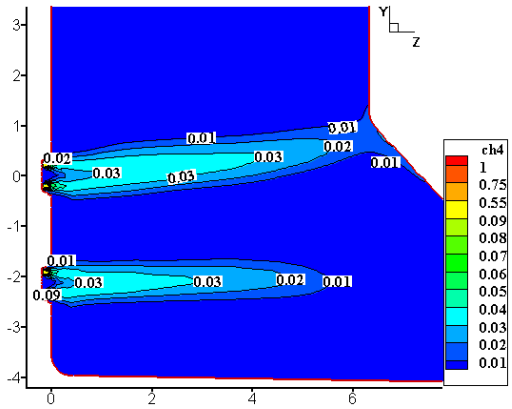


c) Oxyfuel combustion (29%$O_2$ and 71% $CO_2$ by volume)

Figure 6 Contours for mass fraction $CH_4$ of vertical plane passing through burners 2 & 5

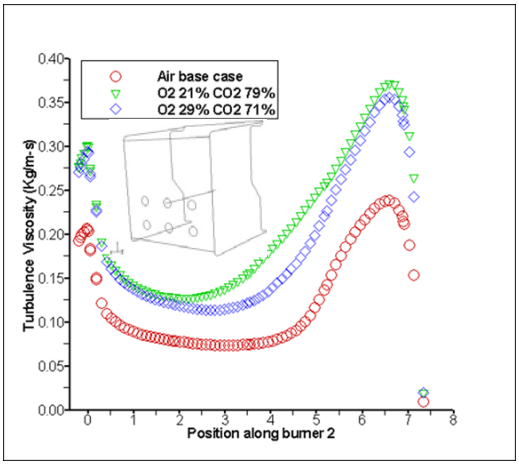


Figure 7a Axial distribution of the turbulent viscosity along the upper middle burner

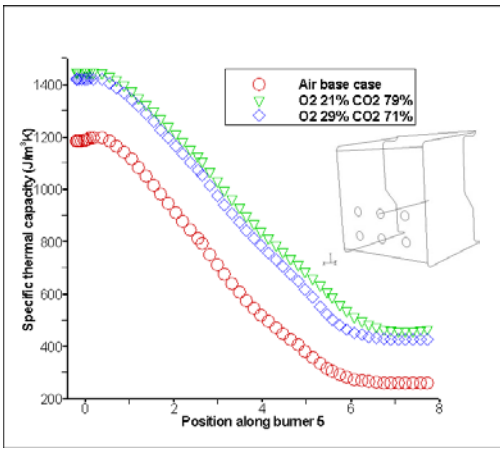


Figure 7b Axial distribution of the specific thermal capacity along the upper middle burner.

The same overall trends are consistent with those of Kiga et al. (1997), who investigated the ignition characteristics of oxyfuel

combustion of pulverized coal in a $CO_2$-rich atmosphere by measuring the flame propagation speed. It was found that the flame propagation speed in $O_2/CO_2$ is lower than that in $O_2/N_2$ environment, and this behavior was attributed to the higher heat capacity of $CO_2$ as compared to that of $N_2$. The higher heat capacity has also been used to explain the delayed flame ignition in oxy-fuel combustion [Kimura 1995 and Kiga et al. 1997]. Flammability limits and flame speeds are affected by the substitution of $CO_2$ for $N_2$ and it was concluded that $CO_2$ has an inhibitory effect on flame propagation and stability. Croiset (2000) reported that flame ignition is delayed in oxyfuel combustion during pilot-scale experiments utilizing pulverized coal combustion in $O_2/CO_2$ mixtures. In order to clarify the impact of oxyfuel combustion on the reduction of the flame temperature and the burning rate, the specific thermal capacity $(\rho C_p)$ for the cases of air-fuel combustion and oxyfuel combustion (replacement of $N_2$ by $CO_2$) were calculated. These results are shown in Fig. 7b providing the distribution of $\rho C_p$ along the axis of the upper middle burner. The figure indicates higher specific thermal capacity in the case of the oxyfuel combustion in comparison to that of air-fuel combustion. This explains the lower temperature levels and flame cooling effects exhibited in the oxyfuel combustion cases. Increasing the $CO_2$ recirculation percentage results in higher specific thermal capacity in the combustion products and resulting in lower temperature levels.

In the case of oxyfuel combustion, the volume of gases flowing through the furnace is reduced because the increase in the density of the flue gas [Buhre et al. (2005)]. This is because the molecular weight of $CO_2$ is 44, compared to 28 for $N_2$. Thus, for the same mass flow rate, the volume flow rate of the gases in oxyfuel combustion is lower than that in case of air-fuel combustion. These observations are confirmed by the flame sizes of the oxyfuel and air-fuel cases obtained in the present study and shown in Fig. 5. Figure 8 shows the contours of the $CO_2$ concentrations, indicating the rise in $CO_2$ levels from around 14% in the case of air-fuel combustion to above 80% in the oxyfuel combustion in most of the furnace volume. The axial distribution of the gas density along the axis of the upper burner is shown in Figure 9. The figure indicates higher density in the case of oxyfuel combustion. This explains the smaller gas volume exhibited in the oxyfuel combustion cases. The figure also indicates that the increase in the percentage of $CO_2$ recirculation results in higher gas density leading to lower radiation rates.

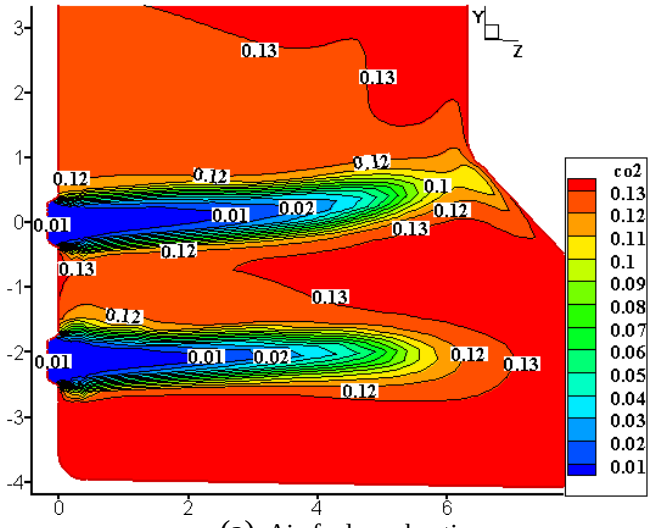


(a) Air-fuel combustion

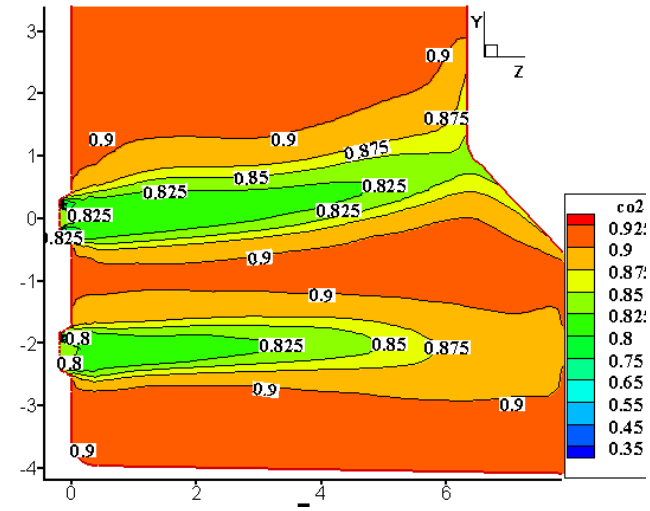


b) Oxyfuel combustion (21%$O_2$ and 79% $CO_2$ by volume)

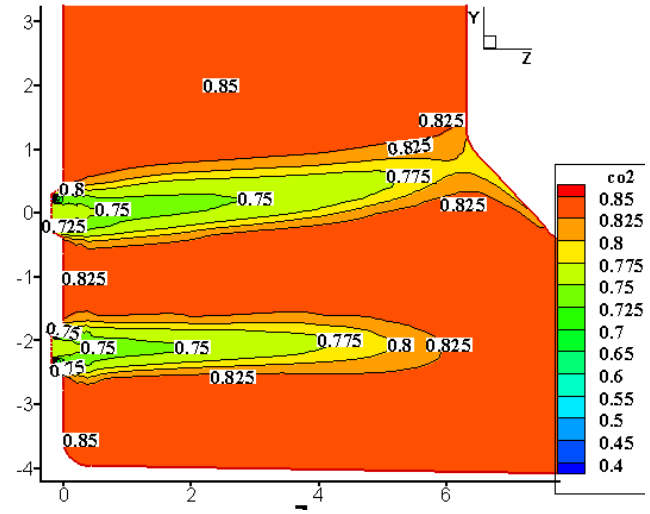


c) Oxyfuel combustion (29%$O_2$ and 71% $CO_2$ by volume)

Figure 8 Contours for mass fraction $CO_2$ of vertical plane passing through burners 2 & 5

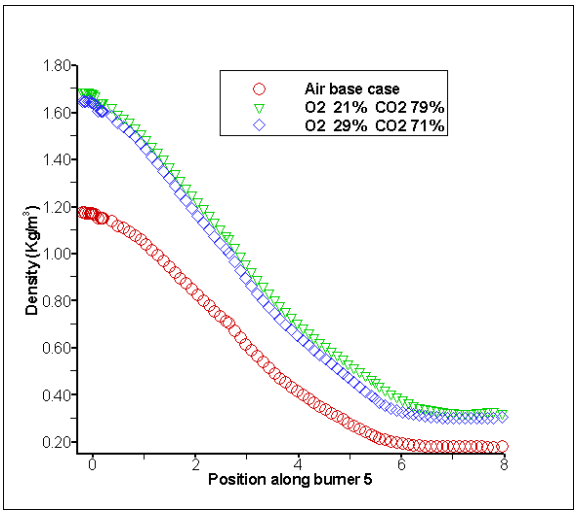


Figure 9 Axial distribution of the density along the upper middle burner

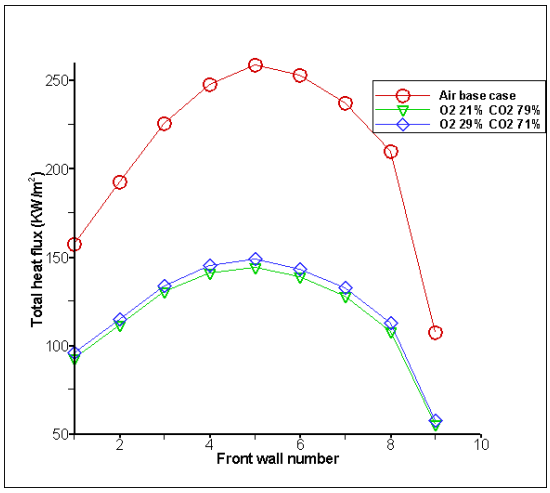


Figure 10a Total heat flux along the front wall of the boiler.

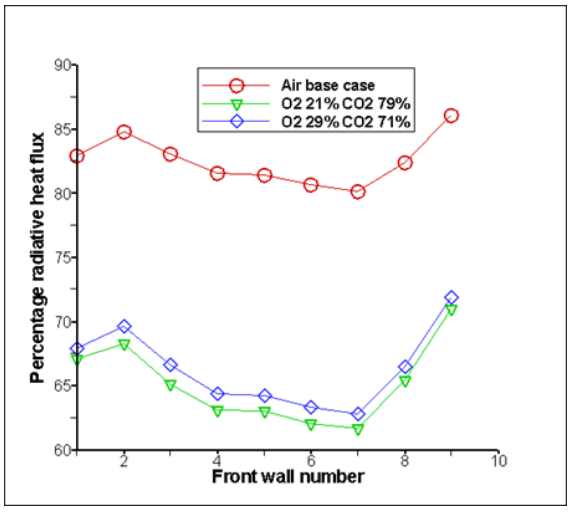


Figure 10b Percentage heat radiation along the front wall of the boiler

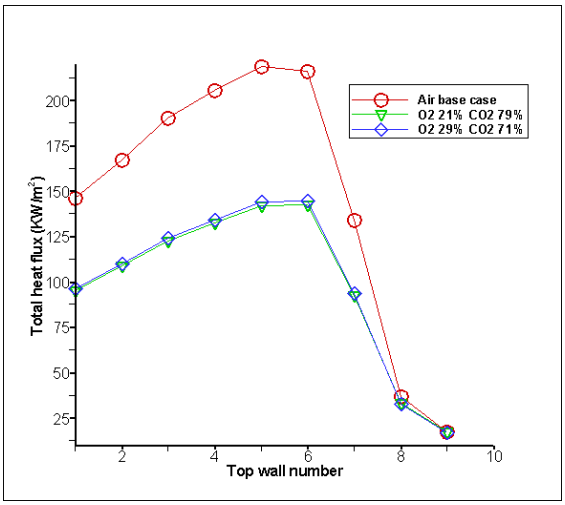


Figure 11a Total heat flux along the top wall of the boiler.

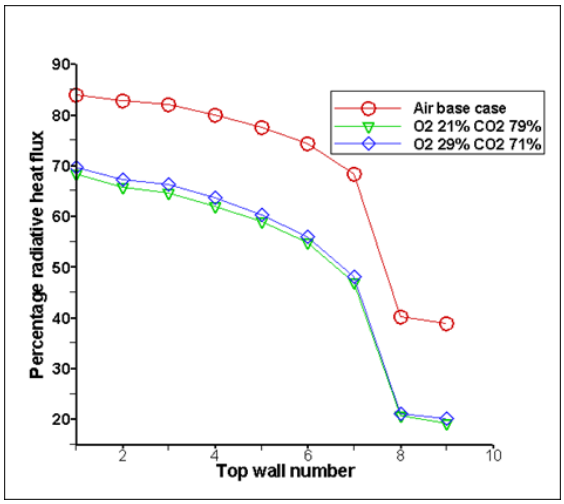


Figure 11b Percentage heat radiation along the top wall of the boiler.

The boiler performance is judged by the heat flux distribution along the different surfaces of the boiler in both sections of the furnace. The characteristics of heat transfer from the burnt gases to the water jacket along the different side and top surfaces shown in Figs 10 and 11 are now discussed in detail. The total energy absorbed and the radiation percentage are much higher in the case of the air-fuel combustion along the whole surface except for the end part close to the furnace rear wall. Figures 11a and 11b present the total heat transfer and radiation percentage along the top part of the furnace and indicate a similar situation as those of the front wall.

## CONCLUSIONS

The thermal characteristics of oxyfuel and air combustion in the furnace of an industrial water tube boiler were investigated and compared to the conventional air-fuel combustion. The influence of the $CO_2$ circulation on the oxyfuel combustion

characteristics was investigated by comparing two cases of oxyfuel and air-fuel combustion. In the first case, the ratio of oxygen in the mixture of $O_2/CO_2$ was 21% by volume and in the second case $O_2$ concentration was 29% by volume. The results indicate that the temperature levels are reduced in the case of oxyfuel in comparison to the air-fuel combustion case. The results show slow rates of consumption of the fuel and oxygen consumption in the oxyfuel combustion case in comparison to the fuel air combustion case. It is also shown that the energy absorbed is much higher in the case of the air fuel combustion along the surfaces It was concluded that the flame propagation speed in $O_2/CO_2$ environment is lower than that in $O_2/N_2$, which was attributed to the higher heat capacity of $CO_2$ compared to that of $N_2$.

**ACKNOWLEDGEMENTS**

The authors wish to acknowlegde the support received from King Abdulaziz City for Science and Technology (KASCT) through The Vice-Rectorship of Applied and Scientific Research at KFUPM under KACST project# AT-29-89.

**REFERENCES**

Andersson, K. and Johnsson, F. (2007), Flame and radiation characteristics of gas-fired $O_2/CO_2$ combustion, Fuel 86, 656–668

Andersson, K. and Johnsson, F., 2006, Radiative properties of a 100 kW oxy-fuel flame experiments and modeling of the Chalmers test facility, Proceedings of Clearwater Clean Coal. Conference, May 2006.

Andersson, K., 2007, Combustion Tests and Modeling of the Oxy-fuel Process, 2nd Workshop on International Oxy-Combustion Research Network, Windsor, CT, USA, 25 – 26 January 2007.

Andersson, K., Johanson, R., Hjärtstam, S., Johnsson, F. and Leckner, B., 2007a, Radiation intensity of lignite-fired oxy-fuel flames, Chem. Eng. Science.

Andersson, K., Johanson, R., Johnsson, F., Leckner, B., 2007b, Radiation intensity of propane-fired oxy-fuel flames: Implications for soot formation, Energy and Fuels.

Attya, A. M. and Habib, M. A., 1990, "The Influence of Spray Characteristics and Air Preheat on the Flame Properties in a Gas Turbine Combustor," Multi-phase Transport and Particulate Phenomena, Edited by T. Nejat Veziroglu, Hemisphere Publishing Corporation, N. Y., Vol. 3, PP. 543-566.

Buhre, B. J. P., Elliott, L. K., Sheng, C.D., Gupta, R. P., Wall, T. F., 2005, Oxy-fuel combustion technology for coal-fired power generation, Progress in Energy and Combustion Science 31, 283–307.

Croiset, E. and Thambimuthu, K. V., 1999, Coal. combustion with flue gas recirculation for $CO_2$ recovery. In: Riemer P, Eliasson B, Wokaun A, editors, Greenhouse gas technologies. Amsterdam: Elsevier Science, pp. 581–586.

Croiset, E., Thambimuthu, K. V. and Palmer, A., 2000, Coal combustion in $O_2/CO_2$ mixtures compared with air. Can J Chem Eng, Vol. 78, pp.402–407.

Ditaranto, M., Hals, J., Thermo-acoustic instabilities in a $CO_2$ diluted oxy-fuel combustor, 2nd Workshop on International. Oxy-Combustion Research Network, Windsor, CT, USA, 25–26 January 2007.

Eriksson, K., CFD modeling for oxyfuel combustion, 2nd Workshop on International. Oxy-Combustion Research Network, Windsor, CT, USA, 25 – 26 January 2007.

Fluent 6.2 User's Guide, 2003, Fluent Inc., Center Research Park, 10 Cavendish Court, Lebanon, NH 03766, USA.

Habib, M. A. and Whitelaw, J. H., 1982, The Calculation of Turbulent flow in wide angle diffusers, Num. Heat Transfer, Vol. 5, pp. 145-164.

Habib, M.A., Attya, A. E. and McEligot, D. M., 1989, Calculation of turbulent flow and heat transfer in channels with streamwise periodic flow, ASME Journal of Turbomachinery, Vol., 110, pp. 405-411.

Kakaras, E., A. Koumanakos, A. Doukelis, A., Giannakopoulos, D., Vorrias, I. (2007), Oxyfuel boiler design in a lignite-fired power plant, Fuel 86, pp. 2144–2150

Khare, S., Wall, T. F., Gupta, R. P., Elliott, L. and Buhre, B., 2005, Oxy-fuel ($O_2/CO_2$, $O_2$/RFG) technology for sequestration-ready CO2 and emission compliance. The Clearwater coal conference: the 30th international technical conference on coal utilization & fuel systems, coal. technology: yesterday – today- tomorrow, Clearwater, USA, April 17–21.

Kiga T, Takano S, Kimura N, Omata K, Okawa M, Mori T, et al. Characteristics of pulverised-coal combustion in the system of oxygen/recycled flue gas combustion. Energy Convers Manage 1997;38:S129–S34.

Kimura K, Omata K, Kiga T, Takano S, Shikisima S. Characteristics of pulverized coal. combustion in O2/CO2 mixtures for CO2 recovery. Energy Convers Manage 1995; 36: 805–8.

Kvamsdal, H. M., 2005, Poer Generation with $CO_2$ management our activities, $CO_2$ Seminar, 22/2/2005, Gas Technology Center NTNU, SINTEF.

Launder, B.E. and D. B. Spalding, 1974, The numerical. computation of turbulent flows, Computer Methods in Applied Mechanics and Engineering, Vol. 3, pp. 269-289.

Liu, F., Becker, H. A. and Bindar, Y., 1998, A Comparative Study of Radiative Heat Transfer Modeling in Gas-Fired Furnaces Using the Simple Grey and the Weighted-Sum-of-Grey-Gases Models. International J. of Heat and Mass Transfer, Vol. 41, pp. 3357-3371

Magnussen, B. F. and Hjertager B. H., 1976, On mathematical models of turbulent combustion with special emphasis on soot formation and combustion, In 16th Symp. (Int'l.) on Combustion, The Combustion Institute, 1976.

Modak, A.T., 1979, Radiation from products of combustion, Fire Research, Vol.1, pp. 339-3361.

Mönckert, P., Reber, D., Maier, J. and Scheffknecht, G., 2007, Operation of a retrofitted 0.5 MWth PF Combustion facility under oxyfuel conditions-An experience report, Proceedings of Clearwater Clean Coal. Conference, Clearwater FL., June 2007.

Mongia, H. C., 46th AIAA Aerospace Sciences Meeting and Exhibit 7 - 10 January 2008, Reno, Nevada AIAA 2008-1445, Recent Progress in Comprehensive Modeling of Gas Turbine Combustion, Mongia, GE Aviation, Cincinnati, Ohio, U.S.A.

Normann, F., Thunman, H., and Johnsson, F., 2009, Process analysis of an oxygen lean oxy-fuel power plant with co-production of synthesis gas, Energy Conversion and Management 50, 279-286

Payne, R., Chen, S. L., Wolsky, A. M. and Richter, W. F., 1989, CO2 recovery via coal combustion in mixtures of oxygen and recycled flue gas.

Raithby G. D. and Chui E. H., 1990, A Finite-Volume Method for Predicting a Radiant Heat Transfer in Enclosures with Participating Media. J. Heat Transfer, Vol. 112, pp. 415-423.

Reynolds, W.C., 1987, "Fundamentals of turbulence for turbulence modeling and simulation," Lecture Notes for Von Karman Institute, Agard Report No. 755.

Rising, B., 2007, Oxyfuel combustion Cycle for $CO_2$ capture, Florida DEP Cenral District Power Generation Conference, July 2007, Orlando, Florida.

Sanz, W., Jericha, H., Luckel, F., Göttlich, E., Heitmeir, F., 2005, A Further Step towards a Graz Cycle Power Plant for a $CO_2$ Capture, Proceedings of GT2005 ASME Turbo Expo 2005: Power for Land, Sea and Air June 6-9, 2005, Reno-Tahoe, Nevada, USA GT2005-68456.

Shaddix, C., Coal particle ignition, devolatilisation and char combustion kinetics during oxy-combustion, 2nd Workshop on International. Oxy-Combustion Research Network, Windsor, CT, USA, 25 – 26 January 2007.

Shah, M. M., Christie, M., Oxy-fuel combustion using OTM for $CO_2$ capture from coal power plants, 2nd Workshop on International. Oxy-Combustion Research Network, Windsor, CT, USA, 25-26 January 2007.

Shih, T.H., W. W. Liou, A. Shabbir, and J. Zhu, 1995, A new k-ε eddy-viscosity model for high Reynolds number turbulent flows - Model development and validation, Computers and Fluids, Vol. 24, No. 3, pp. 227-238.

Shuja, S. Z. and Habib, M. A., 1996, Fluid Flow and Heat Transfer Characteristics in Axisymmetric Annular Diffusers, Computers and Fluids, Vol. 25, No. 2, pp.133-150.

Smith, T. F., Shen, Z. F. and Friedman, J. N., 1982, Evaluation of Coefficients for the Weighted Sum of Gray Gases Model, J. Heat Transfer, Vol. 104, pp. 602-608.

Versteeg, H. K. and Malalasekera, W., 1995, An Introduction to Computational Fluid Dynamics; the Finite Volume Method, Longman Scientific and Technical.

Wall, T. F., 2007, Combustion processes for carbon capture Terry F. Wall, Proceedings of the Combustion Institute, Vol. 31, pp. 31-47

Wall, T.F., Khare, S., Farida, Z., Liu, Y., 2007, Ignition of oxy-fuel flames, 2nd Workshop on International Oxy-Combustion Research Network, Windsor, CT, USA, 25-26 January.

WEC, World Energy Council, 2004, available at <http:// www.worldenergy.org/wec-geis/edc/scenario.asp/> (Access date: October 27, 2004).

Wilcox, D.C., 2000, Turbulence Modeling for CFD, DCW Industries.

Yang, S. L., Y. K. Siow, B. D. Peschke, R. R. Tacina, Numerical. Study of Nonreacting Gas Turbine Combustor Swirl Flow Using Reynolds Stress Model, Vol. 125, JULY 2003 by ASME Transactions of the ASME, pp 804-811

Zanganeh, K., Salvador, C., Mitrovic, M., Modelling, design, and pilot-scale experiments of CANMET's advanced oxy-fuel/stream burner, 2nd Workshop on International. Oxy-Combustion Research Network, Windsor, CT, USA, 25 – 26 January 2007.

Zhang, N. and Lior, N., 2008, Two novel oxy-fuel power cycles integrated with natural gas reforming and $CO_2$ capture. Energy 33, pp.340–351.

Zheng, Y.; Fan, J.; Ma, Y.; Sun, P. and Cen, K., 2000, Computational modeling of Tangentially Fired Boiler II $NO_x$ Emissions, Chinese J. of Chemical Engineering, Vol. 8 (3), pp. 247-250.